

Leadfree perovskite solar cell

Pranjal Sharma, Kunal Lariya, Ghanendra Kumar Joshi, Dipesh Patel

Under the Guidance of:

Prof. Sanjay Kumar Dewangan

Government Engineering College Koni, Bilaspur (C.G.)

Abstract— The growing demand for eco-friendly and high-efficiency solar energy technologies has driven the exploration of lead-free perovskite materials as viable alternatives to traditional lead-based compounds. This project investigates the photovoltaic performance of a novel lead-free chalcogenide perovskite, BaHfS₃, under pressure-tuned conditions (0 GPa and 25 GPa) using SCAPS-1D simulation software. At 25 GPa, BaHfS₃ exhibits a direct bandgap of 1.30 eV — nearly ideal for single-junction photovoltaic applications under the Shockley–Queisser limit. A total of 64 device configurations were tested by varying Electron Transport Layer (ETL) and Hole Transport Layer (HTL) materials. The optimal structure identified was FTO/CdS/BaHfS₃/NiO/Au, achieving a power conversion efficiency (PCE) of 28.71% with a Voc of 0.9591 V, Jsc of 34.42 mA/cm², and FF of 86.98%. Key parameters including absorber layer thickness, doping concentration, defect density, and series/shunt resistance were systematically optimized. The study confirms BaHfS₃ as a sustainable and efficient absorber layer with significant potential for next-generation non-toxic and stable photovoltaic technologies.

Keywords: BaHfS₃, Lead-Free Perovskite, SCAPS-1D, Chalcogenide, Pressure Engineering, ETL, HTL, Power Conversion Efficiency.

I. INTRODUCTION

SCAPS-1D (Solar Cell Capacitance Simulator) developed by ELIS, University of Gent, Belgium, was used for all numerical simulations. The software solves Poisson's equation, and electron/hole continuity equations to model charge transport, generation, and recombination in multilayer photovoltaic structures. Simulations were performed under AM 1.5G illumination (1000 W/m²) at 300 K. The primary device architecture studied is:

FTO / ETL / BaHfS₃ (25 GPa) / HTL / Au

The absorber layer BaHfS₃ was fixed at 800 nm thickness. Eight ETL candidates (TiO₂, WS₂, PCBM, ZnO, CeO₂, IGZO, ZnSe, CdS) and eight HTL candidates (Cu₂O, CuSCN, P3HT, PEDOT:PSS, Spiro-MeOTAD, NiO, CuI, CBTS, CFTS) were evaluated, yielding 64 unique device configurations. Figure 1 shows the SCAPS-1D device structure panel for the best-performing configuration (FTO/CdS/BaHfS₃/NiO/Au).

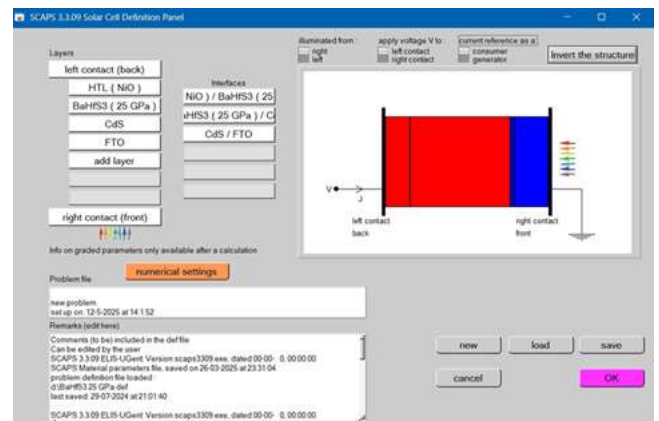


Figure 1: SCAPS-1D Solar Cell Definition Panel – Device structure for FTO/CdS/BaHfS₃ (25 GPa)/NiO/Au

II. PRESSURE-DRIVEN BANDGAP OPTIMIZATION

A critical advantage of BaHfS₃ is its pressure-tunable direct bandgap, which can be optimized for maximum solar absorption. As shown in Table 1, increasing hydrostatic pressure from 0 to 25 GPa reduces the bandgap from 2.11 eV to 1.30 eV, approaching the theoretical optimum of ~1.34 eV for single-junction solar cells. This pressure-induced bandgap narrowing is accompanied by enhanced carrier mobility and

improved optical absorption, making BaHfS₃ under 25 GPa significantly more effective as a photovoltaic absorber.

Pressure (GPa)	Bandgap E _g (eV)
0	2.11
5	2.01
10	1.90
15	1.76
20	1.48
25	1.30 ★

Table 1: Bandgap of BaHfS₃ under increasing hydrostatic pressure (★ = optimal for PV)

III. HIGHEST EFFICIENCY SIMULATION RESULTS (25 GPa)

Out of 64 configurations tested at 25 GPa, nine devices consistently achieved PCE values exceeding 28.50%. Table 2 presents their full performance parameters. The best-performing configuration, FTO/CdS/BaHfS₃/NiO/Au, achieved a peak PCE of 28.71%, enabled by excellent band alignment between CdS (ETL) and NiO (HTL) with the BaHfS₃ absorber, minimizing recombination losses.

PV Cell Configuration	V _{oc} (V)	J _{sc} (mA/cm ²)	FF (%)	PC E (%)
FTO/CdS/BaHfS ₃ /NiO/Au ★	0.9591	34.413	86.98	28.71
FTO/ZnSe/BaHfS ₃ /NiO/Au	0.9586	34.421	86.92	28.68
FTO/ZnSe/BaHfS ₃ /CBTS/Au	0.9554	34.430	86.86	28.68
FTO/CdS/BaHfS ₃ /CBTS/Au	0.9591	34.419	86.98	28.71

FTO/IGZO/BaHfS ₃ /CBTS/Au	0.9587	34.410	86.59	28.56
FTO/IGZO/BaHfS ₃ /NiO/Au	0.9585	34.403	86.59	28.56
FTO/CdS/BaHfS ₃ /Spiro/Au	0.9558	34.412	86.73	28.53
FTO/ZnSe/BaHfS ₃ /Spiro/Au	0.9555	34.421	86.66	28.50
FTO/IGZO/BaHfS ₃ /Spiro/Au	0.9554	34.403	86.35	28.38

Table 2: Top 9 high-efficiency device configurations at 25 GPa (★ = best performing)

IV. J-V CHARACTERISTICS & QUANTUM EFFICIENCY

Figure 2 shows the J–V characteristic and recombination current analysis for the best configuration (FTO/CdS/BaHfS₃/NiO/Au) as obtained directly from SCAPS-1D. The simulation clearly shows the characteristic solar cell behavior with V_{oc} = 0.9584 V, J_{sc} = 34.32 mA/cm², FF = 86.68%, and η = 28.52%. The near-square J–V curve reflects excellent fill factor performance and low internal recombination losses.

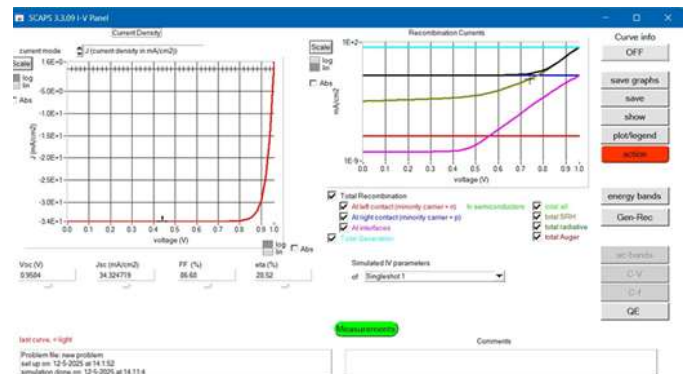


Figure 2: SCAPS-1D J–V characteristics for FTO/CdS/BaHfS₃ (25 GPa)/NiO/Au — V_{oc} = 0.9584 V, J_{sc} = 34.32 mA/cm², FF = 86.68%, PCE = 28.52%

Figure 3 presents the Quantum Efficiency (QE) spectrum of the optimal device, demonstrating near-100% absorption efficiency across the 350–850 nm wavelength range. The broad and flat QE curve confirms superior light harvesting capability

of BaHfS₃ at 25 GPa, with the gradual roll-off beyond 850 nm corresponding to photons approaching the bandgap energy of 1.30 eV.

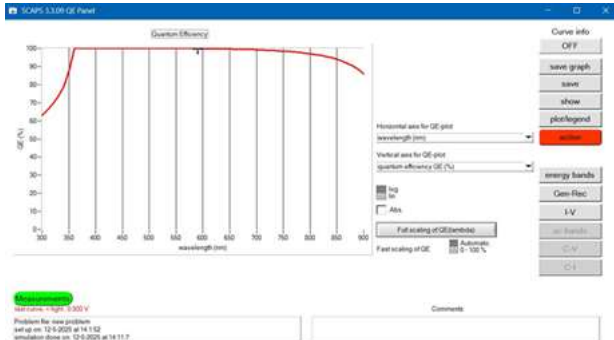


Figure 3: Quantum Efficiency (QE) spectrum — near-100% QE across 350–850 nm confirms broad-spectrum absorption

V. ENERGY BAND DIAGRAM & CARRIER ANALYSIS

Figure 4 shows the SCAPS-1D energy band diagram and carrier density profiles for the optimal device structure. The band diagram confirms proper band alignment across the FTO/CdS/BaHfS₃/NiO/Au heterostructure, ensuring efficient photogenerated carrier separation and collection. The carrier density plot shows that photogenerated holes and electrons are effectively swept toward their respective contacts, confirming minimal interfacial recombination in the optimized device.

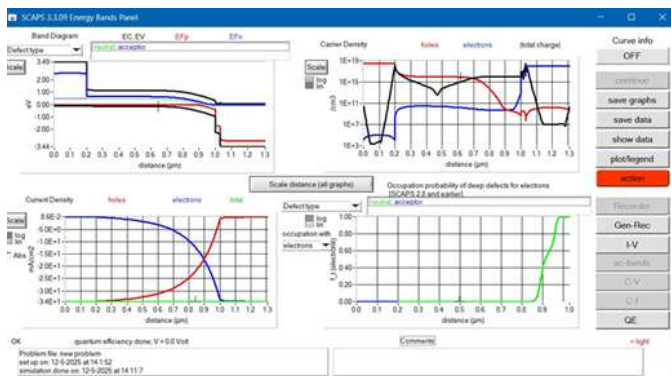


Figure 4: Energy band diagram, carrier density, and current density profiles (SCAPS-1D) for the optimal device structure

VI. ABSORBER LAYER OPTIMIZATION

The influence of absorber thickness (0.7–1.4 µm) and shallow acceptor density Na (10¹⁶–10²¹ cm⁻³) was investigated via 2D contour maps. Key findings are:

Parameter	Optimum Condition	Peak Value Observed
PCE (η)	Na ≈ 10 ²¹ cm ⁻³ , thickness ≈ 1.4 µm	≈ 39.15%
Fill Factor (FF)	High Na (≥10 ²¹ cm ⁻³)	≈ 90%
Jsc	Thickness ≥ 1.2 µm (light absorption)	≈ 35.35 mA/cm ²
Voc	High Na (≥10 ¹⁹ cm ⁻³)	≈ 1.247 V

Table 3: Absorber optimization summary — effect of thickness and acceptor density (Na) at 25 GPa

VII. COMPARATIVE ANALYSIS: 0 GPa vs 25 GPa

Table 4 presents the top 9 results at 0 GPa (without pressure), alongside the 25 GPa results, demonstrating the transformative impact of pressure tuning. At 0 GPa, the bandgap of 2.11 eV results in reduced Jsc and an overall PCE limited to ~15.80%, while at 25 GPa the narrowed bandgap of 1.30 eV dramatically boosts both Jsc and overall PCE to 28.71%.

Configuration	Pressure (GPa)	Voc (V)	Jsc (mA/cm ²)	FF (%)	PCE (%)
FTO/CdS/BaHfS ₃ /CBTS/Au	25 GPa	0.9591	34.419	86.98	28.71
FTO/IGZO/BaHfS ₃ /CBTS/Au	25 GPa	0.9587	34.410	86.59	28.56
FTO/ZnSe/BaHfS ₃ /CBTS/Au	25 GPa	0.9554	34.430	86.86	28.68

FTO/CdS/BaHfS ₃ /NiO/Au	25 GPa	0.9591	34.413	86.98	28.71
FTO/CdS/BaHfS ₃ /CBTS/Au	0 GPa	1.4600	12.178	88.84	15.80
FTO/IGZO/BaHfS ₃ /CBTS/Au	0 GPa	1.4596	12.167	88.62	15.74
FTO/CdS/BaHfS ₃ /NiO/Au	0 GPa	1.3563	11.050	86.60	12.98
FTO/IGZO/BaHfS ₃ /NiO/Au	0 GPa	1.3557	11.035	86.23	12.90
FTO/ZnSe/BaHfS ₃ /NiO/Au	0 GPa	1.3563	11.031	86.38	12.92

Table 4: Performance comparison of best configurations at 0 GPa (amber) vs 25 GPa (green)

VIII. CONCLUSION

This project successfully demonstrated that pressure-engineered BaHfS₃ is a highly promising lead-free absorber material for perovskite solar cells. Using SCAPS-1D simulation across 64 device configurations, the optimal architecture FTO/CdS/BaHfS₃ (25 GPa)/NiO/Au was identified, achieving a peak power conversion efficiency of 28.71% — significantly higher than the 15.80% obtained at ambient pressure. The study confirms that pressure tuning effectively reduces the bandgap from 2.11 eV to 1.30 eV, enhancing both photon absorption and carrier mobility. CdS and ZnSe emerged as the most effective ETL materials, while NiO and CBTS proved superior as HTL materials due to favorable band alignment and reduced recombination. Absorber optimization further revealed that higher doping concentrations ($\geq 10^{20} \text{ cm}^{-3}$) and thicker absorber layers ($\geq 1.2 \mu\text{m}$) maximize device performance. These findings contribute meaningfully to the development of next-generation non-toxic, stable, and high-efficiency photovoltaic technologies.